JOURNAL OF MATERIALS SCIENCE 27 (1992) 5–12

Alumina scale growth at zirconia–MCrAlY interface: a microstructural study

L. LELAIT, S. ALPÉRINE, R. MÉVREL
ONERA Materials Science Department, BP 72, 92322 Châtillon Cedex, France

High-temperature oxide scale growth at the ceramic–metal interface is a major contributor to the thermomechanical resistance of thermal barrier coatings for hot stages of gas turbines. In order to better understand this phenomenon, microstructural observations of the alumina scales formed at 1100 and 1200 °C under air, between low-pressure plasma-sprayed NiCrAlY and air plasma-sprayed ZrO_2–8.5 wt % Y_2O_3, have been performed by classical and analytical transmission electron microscopy on transverse thin foil specimens. The evolution of the oxide grain morphology from the metal–oxide to the oxide–oxide interface suggests that the scale growth principally takes place at the metal–oxide interface. Segregation of yttrium at oxide grain boundaries has been detected as well as significant quantities of zirconium inside the alumina grains. The oxide growth seems to be dominated by a classical grain-boundary oxygen diffusion mechanism. The presence of zirconium inside the alumina grains also suggests that Al_2O_3 partially forms by chemical reduction of ZrO_2 by Al. The comparison between the microstructures observed and that of alumina scales grown under similar conditions on bare MCrAlY alloys gives some insight into how the ceramic top-coat modifies NiCrAlY high-temperature oxidation mechanisms.

1. Introduction

One of the critical requirements for the application of thermal barrier coatings on hot-stage turbine components is a high bond strength between the metallic bond coat and the ceramic overlayer [1]. In the case of yttria–partially stabilized zirconia (YPSZ) top-coat plasma sprayed on a metallic bond coat, oxide scale growth at the ceramic–metal interface is a major contributor to the interfacial thermomechanical resistance of the coating. Plasma-sprayed MCrAlY layers (M = Ni and/or Co) have been widely used as high-temperature resistant coatings to lengthen the service life of gas turbine parts operating under an oxidizing atmosphere, and in some cases, in the presence of corrosive liquid phases such as sulphates [2]. They are widely used as thermal barrier bond coats, advantage being taken not only of their oxidation resistance, but also of their high-temperature plasticity [3]. Although the intrinsic oxidation resistance of MCrAlY alloys has been the subject of numerous papers [4–6], it is to be noted that only limited efforts [7, 8] have been dedicated to the study of the interfacial oxide scale growth at the ceramic–MCrAlY interface of thermal barrier coatings.

In fact, one can imagine more than one reason why the presence of a ceramic top-coat would alter the oxidation mechanism of MCrAlY alloys: the ceramic top-coat could lower the value of the oxygen pressure (P_{O_2}) at the oxide scale external surface; zirconia top-coats could also be a secondary source of Y diffusion (and primary source of Zr diffusion) in the growing oxide scale, thereby modifying the boundary conditions for the well-known "active element effect". On these grounds, it is interesting to examine if and how the presence of a zirconia top-coat modifies the oxide scale growth mechanisms on MCrAlY alloys. For this purpose, a study was initiated to investigate the microstructure of alumina scales formed by oxidation of YPSZ thermal barrier coatings and to compare it with published data concerning alumina scales grown under similar conditions on a bare MCrAlY alloy [4, 5]. The microstructure of the oxide scales was principally studied by transmission electron microscopy on transverse thin foils. The evolution of the size and morphology of the oxide grains was particularly looked at, since it constitutes an indication of the scale growth mechanisms (diffusing species). Analytical studies were also performed with the hope to observe an eventual diffusion of zirconium and/or yttrium in the oxide grains or grain boundaries, whether coming from the metallic bond-coat or the zirconia top-coat.

2. Experimental procedure

The substrates used were 25 mm × 40 mm × 2 mm coupons of Hastelloy X superalloy (Ni–22Cr–18.5Fe–6Ta–9Mo–1.5Co–0.6W–0.1C–0.5Si, wt %), which were sand-blasted (Al_2O_3 220 mesh, 2 bar) and degreased (vapour-phase trichloroethylene). The substrates were first coated with a 100 μm thick Ni–23Cr–6Al–0.5Y (wt %, Amdry 963) alloy deposited by low-pressure plasma spraying. These samples were then heat-treated for 4 h at 1080 °C under secondary vacuum for bond-coat diffusion and covered

0022–2461/92 $03.00 + .12

with a 300 μm thick layer of air plasma-sprayed ZrO_2–8.5 wt % Y_2O_3 (MEL SCZ8). Plasma spraying operations were performed by Heurchrome. Oxidation of the specimens was obtained during 100 h annealing at 1100 and 1200 °C in air followed by air-quenching.

Transverse thin foils for transmission electron microscopy (TEM) were prepared following a procedure derived and adapted from that described by King *et al.* [9]. The preparation involves four steps: sample embedding, coarse sectioning, mechanical thinning, and final thinning to electron transparency. Initially thin plates (3 mm × 2 mm × 50 mm) – rendered conducting by an electroless silver layer a few micrometres thick – were embedded into electrodeposited nickel (thickness 500 μm). The samples were then sliced into 400 μm thick discs using a diamond wafering blade. Each specimen was thinned to 100 μm and then mechanically prethinned to 20–30 μm using a "Dimpler". After mechanical prethinning, the sample was then thinned by ion-beam bombardment (Ion Tech, Supermicrolap Mark 2) at an incident angle of 17° until perforation occurred. This procedure is described in full detail elsewhere [10]. Jeol 200CX and 4000FX microscopes (the latter equipped with a scanning transmission STEM unit) were used to observe three regions across the oxide layer: near the oxide–zirconia interface, in the central zone of the scale, and near the oxide–NiCrAlY interface. In each case, the distributions of the alumina grain sizes and anisotropy were determined by image analysis routines from a population of at least 100–150 grains. Grain size determination refers to the diameter of equivalent circular grains (computed from an area/perimeter ratio); anisotropy of the grains refers to the ratio of their Feret radii.

Chemical microanalysis was performed on the thin foils by energy-dispersive spectroscopy (EDS) with a Kevex device equipped with a "quantum" diode, using a probe diameter of about 10 nm. In addition, a Gatan 666 magnetic prism spectrometer for simultaneous parallel electron energy loss spectroscopy (PEELS) was used. All such measurements were made in the diffraction mode, with a collecting angle β of 15.0 mrad. The recorded spectra were calibrated for cell collecting efficiency following standard procedures; background was subtracted by a least-squares fitting procedure, to an exponential decay. Finally, elementary microanalysis was performed using a genuine high sensitivity and high spatial resolution ion-probe instrument (for secondary ion mass spectroscopy (SIMS) with a probe diameter of ~ 80 nm) designed at ONERA. The general description of this instrument and its performances can be found elsewhere [11].

3. Results

During annealing an α-alumina scale grows between the NiCrAlY bond-coat and the zirconia top-coat. After 100 h at 1100 °C or 1200 °C the thickness of the scale is 4 ± 0.5 μm or 6 ± 0.5 μm, respectively.

3.1. Oxide scale morphology and microstructure

Typical bright-field micrographs of the alumina scale grown at 1200 °C and representative of its inner region (close to the NiCrAlY–Al_2O_3 interface) can be seen in Fig. 1a. Micrographs taken in the median and external regions (close to the zirconia–Al_2O_3 interface) can be seen in Fig. 1b and c, respectively. The morphology of the oxide scale significantly changes throughout its thickness. Close to the NiCrAlY, the alumina grains are elongated (typical aspect ratio between 2 and 4), columnar, and display numerous intergranular pores, whereas near the Al_2O_3–ZrO_2 interface they are more isotropic (typical aspect ratio between 1 and 2) and pore-free. The same evolution of grain morphology can be observed for samples annealed at 1100 °C; smaller grains are however present in the latter case (Fig. 2).

In the inner region of the alumina scale, besides the microvoids mentioned above, defects such as dislocation pile-ups can be seen, as well as low-angle grain boundaries (Fig. 1d). Very fine spinel oxides ($Ni(Al,Cr)_2O_4$ according to selected-area diffraction measurements and EDS analysis) have also been detected in this region. At the zirconia–alumina interface there is a fine, dense microstructure of small equiaxial grains (Fig. 1c): $(Al,Cr)_2O_3$, $Ni(Al,Cr)_2O_4$ spinels and NiO. Inside these alumina grains, small round ZrO_2 inclusions are observable (identified by EDS). They are associated with small cubic zirconia grains already present in the as-sprayed specimen. The coexistence of zirconia grains with aluminium-based oxides is a consequence of the "roughness" of the ZrO_2–Al_2O_3 interface.

3.2. Alumina grain size distribution

The distributions of grain sizes determined from TEM observations are reported in Fig. 3; they show that the average grain size regularly increases from the scale external surface to the oxide–metal interface. After 100 h at 1100 °C or 1200 °C, the distribution of alumina grains near the alumina–zirconia interface is relatively sharp, the grain sizes varying from 0.01–0.08 μm or 0.02–0.25 μm, respectively. In the inner region, the size distribution is more scattered, the size limits being 0.02 and 0.35 μm or 0.04 and 1.00 μm, respectively. A qualitative comparison between these values and published data concerning the grain size distribution of an alumina scale grown by oxidation at 1100 °C during 100 h on a bare Ni–24Co–23Cr– 7.8Al–0.2Y wt % alloy [4, 5] is possible (although the MCrAlY composition somewhat differs from ours). The average grain size in the latter case is significantly higher than in the former one. In fact, as can be seen from Fig. 3, the grain size distribution of the oxide grown on bare NiCoCrAlY at 1100 °C is very similar to that of the oxide scale grown at 1200 °C at the NiCrAlY–zirconia interface.

3.3. Chemical microanalysis

Chemical microanalysis experiments (EDS and SIMS)

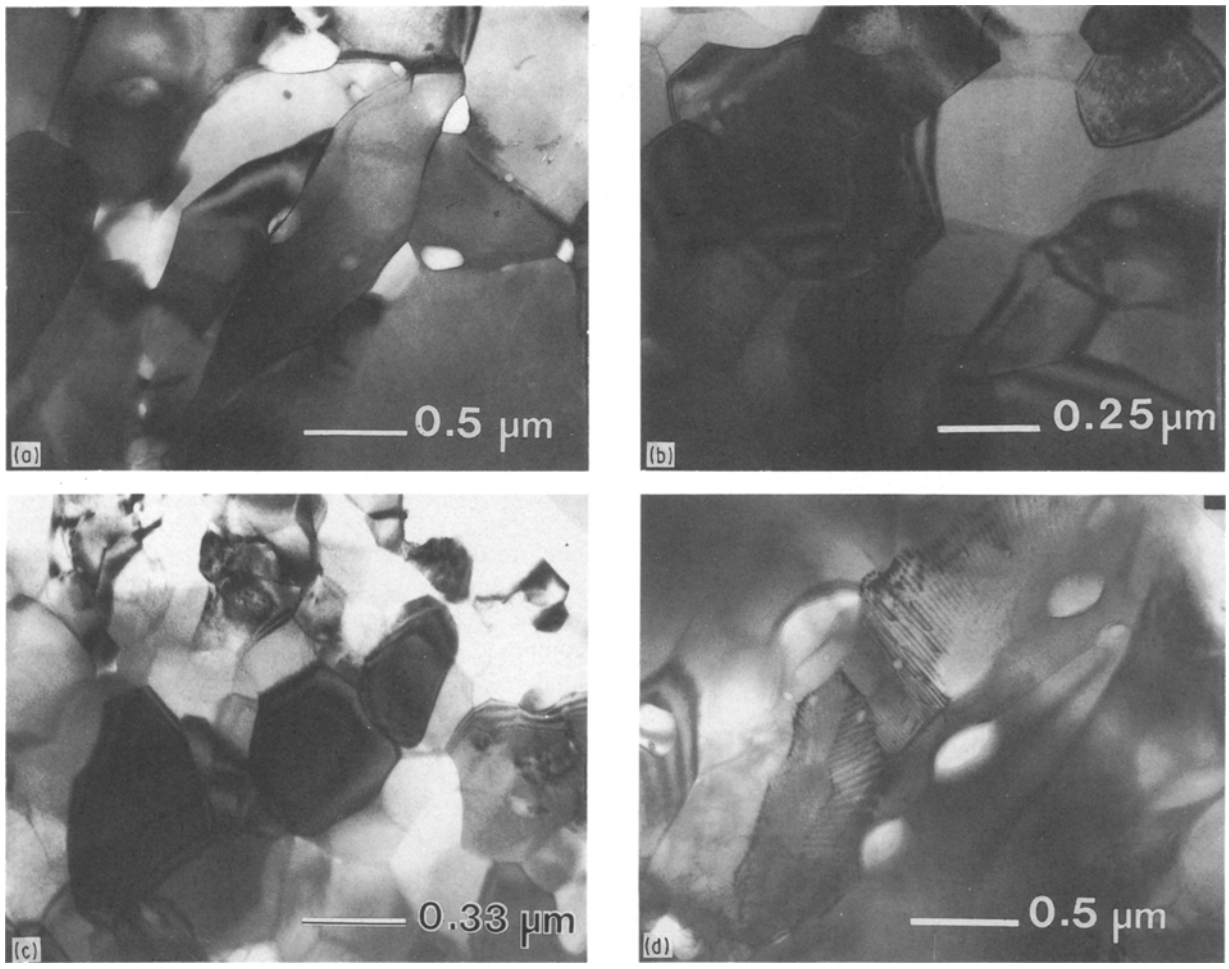

Figure 1 Microstructure of the alumina scale grown during 100 h at 1200 °C: (a) near the NiCrAlY–Al_2O_3 interface, (b) median zone, (c) near the Al_2O_3–ZrO_2 interface, (d) typical defects near the NiCrAlY–Al_2O_3 interface.

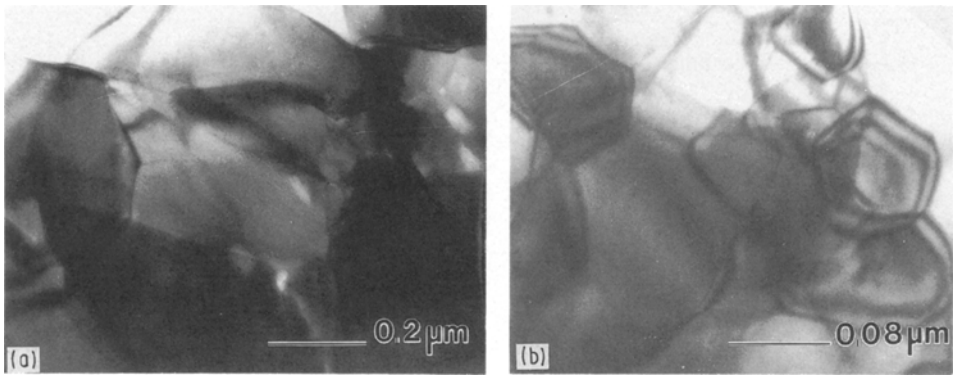

Figure 2 Microstructure of the alumina scale grown during 100 h at 1100 °C: (a) near the NiCrAlY–Al_2O_3 interface, (b) near the Al_2O_3–ZrO_2 interface.

show that the oxide scale grown at 1200 °C at the zirconia–NiCrAlY interface is not composed of pure α-alumina. The alumina scale is bordered, on the NiCrAlY side, by a fine layer of pure chromia (~ 0.25 μm thick), as evidenced by EDS (Fig. 4) as well as by SIMS (see Fig. 9b below). Moreover, most Al_2O_3 grains contain small amounts of chromium (in the order of 1 wt %).

The presence of zirconium is detected almost everywhere in the alumina scale (see the EDS spectrum in Fig. 5), both in the bulk of the oxide grains and in the oxide grain boundaries (within the limitation of a 10 nm EDS probe). The fact that the edge of zirconium is also observed by PEELS (Fig. 6) confirms that the Zr signal detected by EDS is not merely due to the fluorescence of Zr from the nearby zirconia coating. A rough estimate of the zirconium content in the Al_2O_3 grains (using the thin-foil approximation) is about 1 wt %. It is worth pointing out that the zirconium content decreases further with distance from the alumina–zirconia interface.

Fig. 7a and b present detailed energy-dispersive X-ray spectra around the high-energy Y and Zr peaks, collected from regions near the NiCrAlY–Al_2O_3 and

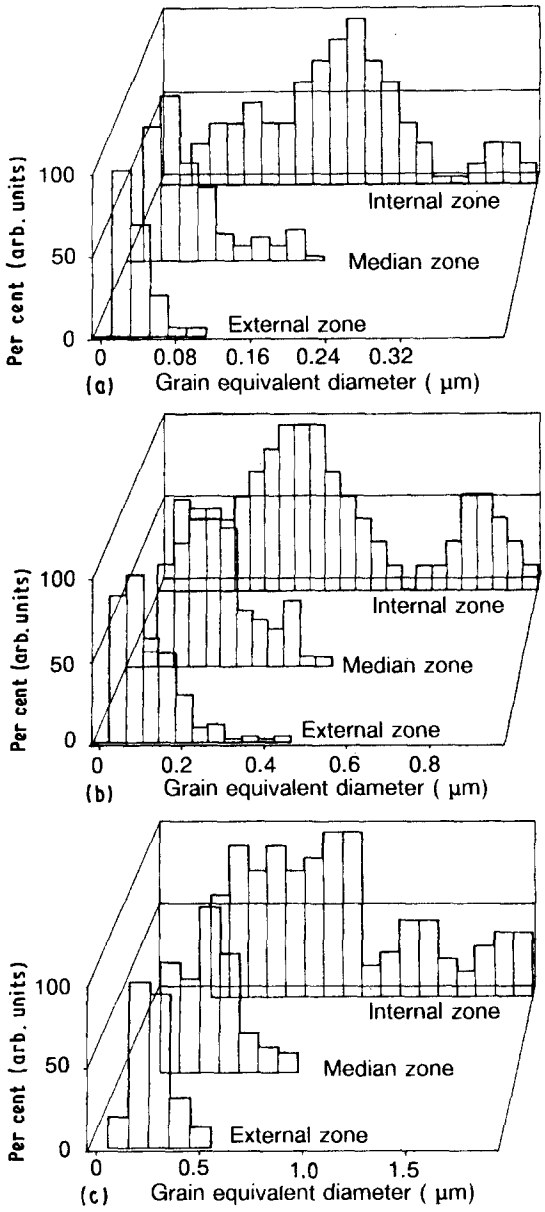

Figure 3 Histograms of grain size distribution: (a) 100 h at 1100 °C, (b) 100 h at 1200 °C, (c) 100 h at 1100 °C on bare NiCoCrAlY alloy (from [4, 5]).

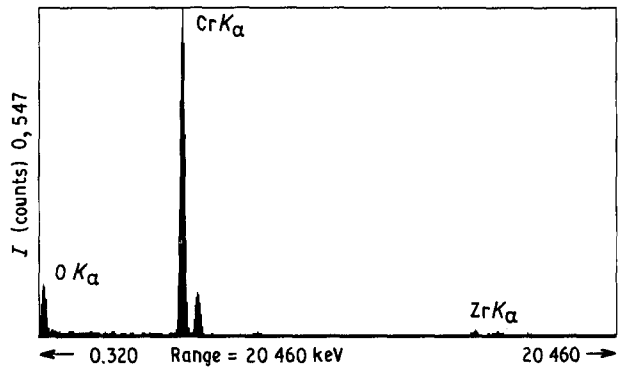

Figure 4 100 h at 1200 °C: EDS analysis of a chromia grain near the NiCrAlY–oxide interface.

Al_2O_3–zirconia interfaces, respectively. In each figure one can see the superimposition of two spectra: one recorded with the 10 nm probe centred in the bulk of a grain, the other one with the probe across a grain boundary. On the NiCrAlY side of the alumina scale

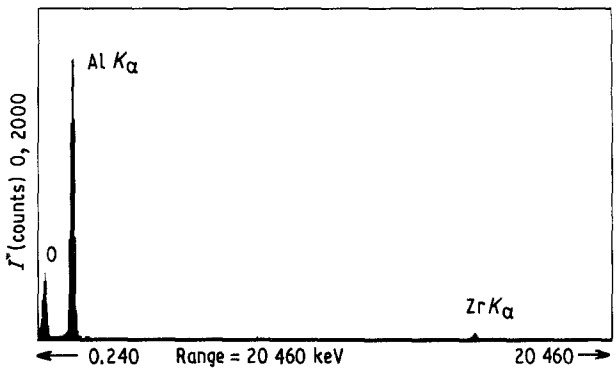

Figure 5 EDS analysis in an alumina grain, showing the presence of zirconium inside the scale.

(Fig. 7a), a yttrium signal is clearly visible, strongly reinforced in the grain boundary. On the other side of the alumina scale (Fig. 7b), no such reinforcement is visible. Even though the size of the probe is large compared to the thickness of the grain boundary analysed, this experiment unambiguously reveals yttrium segregation at the oxide grain boundary near the NiCrAlY–Al_2O_3 interface: the yttrium concentration as indicated by this analysis is of course lower than the real yttrium concentration inside the grain boundary, because of the probe-size smearing effect. The presence of yttrium in the oxide scale is also detected in the form of small $Y_3Al_5O_{12}$ garnets lying in some grain boundaries of the inner region (Fig. 8). Some coarser particles can be seen on the SIMS yttrium map (Fig. 9c). The range of yttrium segregation is, however, too narrow to be properly imaged by SIMS, even with a high spatial resolution (probe size $\sim$ 80 nm).

4. Discussion

The principal microstructural features of the alumina scales grown at the ZrO_2–NiCrAlY interface are schematically represented in Fig. 10. The mechanisms of formation of the oxide scale in our NiCrAlY–YPSZ system can be discussed on the basis of these microstructural observations and also from a comparison between the microstructures of the oxide scale grown on the duplex system and on bare MCrAlY [4, 5]. The structural modifications which could be attributed to the presence of a zirconia top-coat essentially consist of a modification of the grain size distribution inside the oxide scale (smaller grains) and inward diffusion of zirconium (and to a lesser extent yttrium) inside the alumina grains. The microstructure of the oxide scales grown at the zirconia–NiCrAlY interface needs to be discussed in terms of oxide growth mechanisms, oxide composition and scale plasticity.

4.1. Alumina growth mechanisms

The presence of large elongated grains near the metal–oxide interface indicates that the oxide growth occurs predominantly at this interface (at 1100 °C as well as at 1200 °C), and hence that oxygen diffusion through the Al_2O_3 layer is faster than aluminium diffusion. It also leads us to think that yttrium

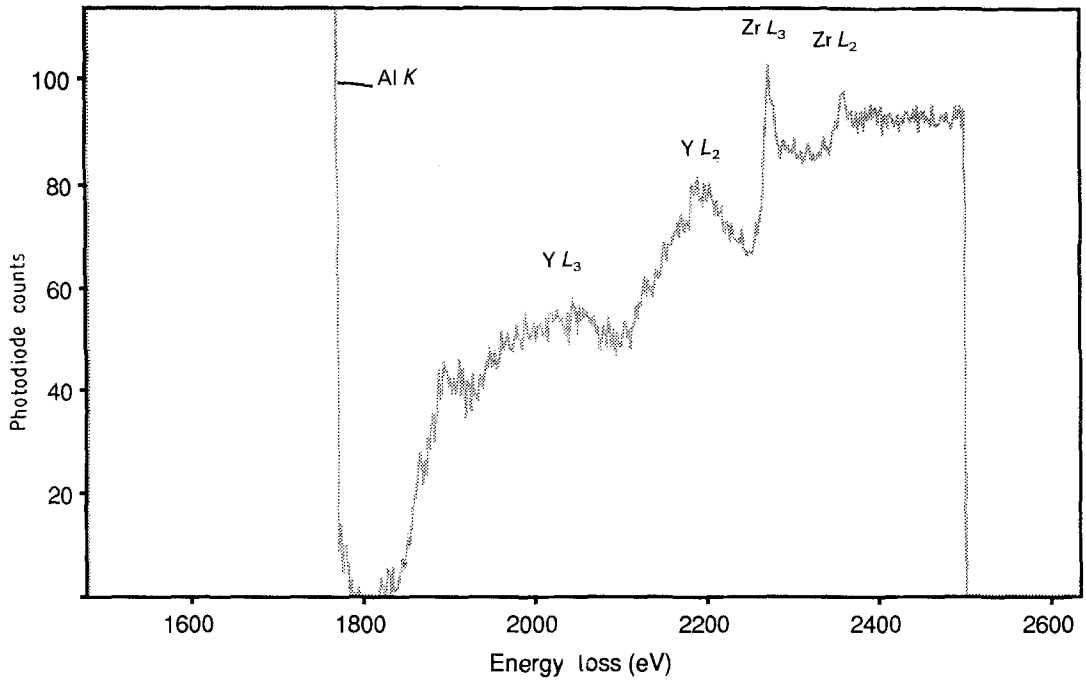

Figure 6 PEELS spectrum recorded inside an alumina grain showing the L_2 and L_3 edges of zirconium and, to a lesser extent, those of yttrium.

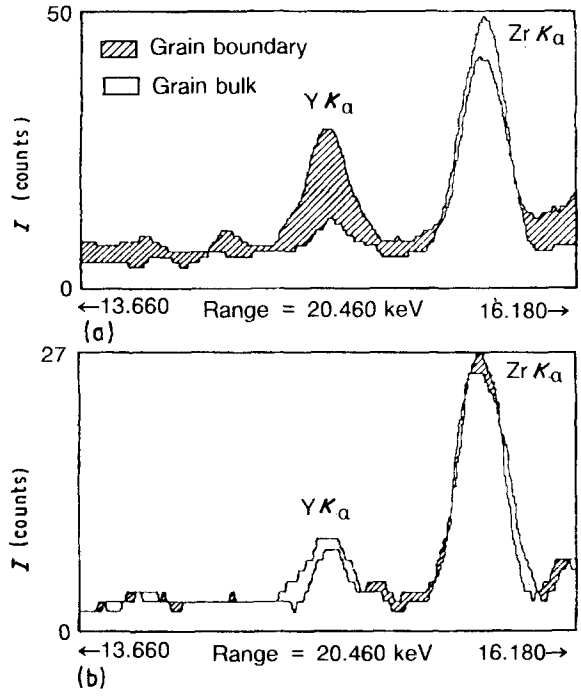

Figure 7 EDS spectra in the Y and Zr high-energy peak region; superimposition of spectra recorded under similar conditions in the grain bulk and at a grain boundary (a) near the NiCrAlY–Al_2O_3 interface, (b) near the Al_2O_3–ZrO_2 interface.

segregation in the oxide grain boundaries – either as $Y_3Al_5O_{12}$ precipitates or on a finer scale – enhances oxygen diffusion at the oxide grain boundaries (Al diffusion in the grain volume being slow). This assumption was first made by Choquet [12], although he could not detect yttrium segregation on oxide thin foils by EDS, due to instrumental limitations.

In the case of oxide growth at an MCrAlY–zirconia interface, however, this oxide growth mechanism could well not be the only one involved. The presence

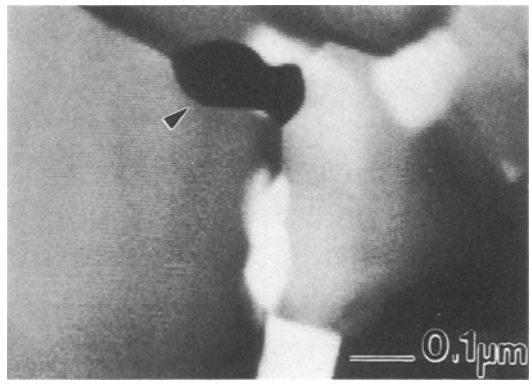

Figure 8 $Y_3Al_5O_{12}$ garnet at a grain boundary in the inner region; STEM imaging.

of significant amounts of zirconium (and lesser amounts of yttrium) inside the oxide layer, with a positive concentration gradient from the inner to the outer part of the oxide scale, shows that, at 1100 and 1200 °C, part of the alumina layer has formed by reduction of the partially stabilized zirconia layer, which is thermodynamically allowed at these temperatures (at 1200 °C, $\Delta G_{ZrO_2} = -816\,kJ\,mol^{-1}$ $O_2 \lesssim \Delta G_{Al_2O_3} = -802\,kJ\,mol^{-1}$ O_2). Zirconium and yttrium atoms thus "trapped" in the alumina layer can further diffuse towards the inner zone of the scale. The presence of zirconium-rich precipitates near the interface suggests that the solubility limit of impurity in α-Al_2O_3 is locally reached here. This secondary growth mechanism, which takes place at the oxide–zirconia interface, is probably of limited extent (as indicated by the grain morphology typical of a scale growth at the metal–oxide interface), since it is limited by the slow volume diffusion of Al atoms through the oxide scale.

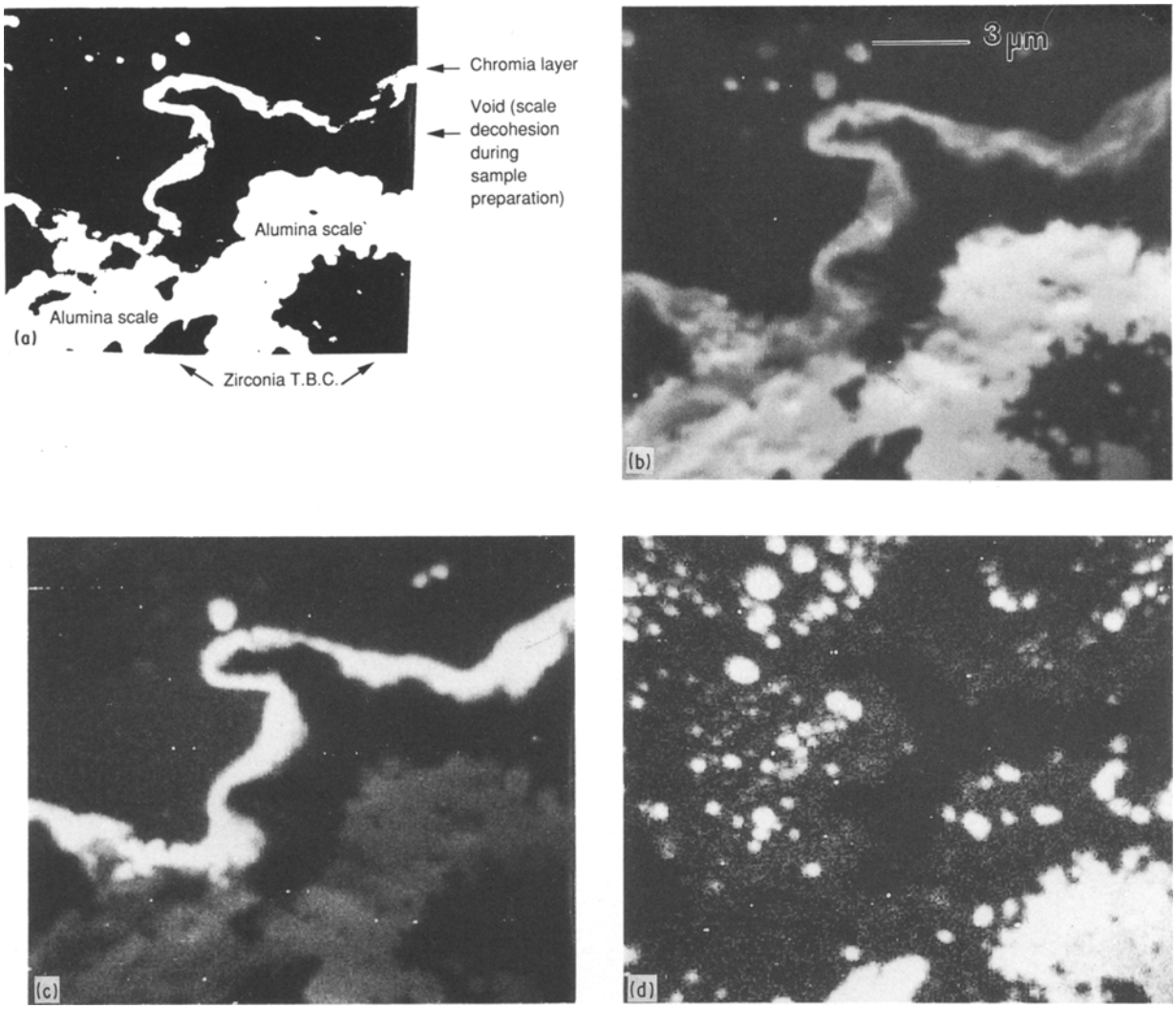

Figure 9 SIMS imaging of the oxide scale grown during 100 h at 1200 °C: (a) schematic drawing showing the topology of the scale, (b) AlO^- secondary ion image, (c) CrO^- image, (d) YO^- image.

4.2. Other oxides

The presence of a thin chromia layer at the NiCrAlY–oxide interface, after 100 h at 1200 °C, is also somewhat unexpected (Cr_2O_3 being less stable than Al_2O_3 at this temperature). It probably forms at the end of the oxidizing treatment after significant aluminium depletion of the NiCrAlY has taken place, preventing any further formation of a continuous alumina layer. This argument is supported by the relatively low initial aluminium content of the bond-coat alloy (6.5 wt %) and by TEMEDS measurements in the NiCrAlY near the metal–oxide interface (confirming significant aluminium depletion during Al_2O_3 scale formation). Some chromium has also diffused and partially substitutes for aluminium in the Al_2O_3 grains.

Other oxides than alumina and chromia have been identified in the oxide scale. The presence of nickel oxides and very small spinels in the outermost region of the scale is not surprising: they were formed during the early stages of oxidation, when a stationary oxidation regime is not yet established, and pushed back as the oxide growth proceeds. On the other hand, the presence of $NiAl_2O_4$ spinels near the MCrAlY–oxide interface is not so easily explained. One notices that the small spinel grains are localized in convoluted regions of the alumina scale. This spinel formation could be a local Al depletion in an alumina-encapsulated metallic "pouch".

4.3. Plasticity

The presence, in relatively large quantities, of dislocation pile-ups inside the oxide scale grown at 1100 and 1200 °C is not easy to interpret. Choquet and co-workers [4, 5] demonstrated that the high value of residual stresses ($\sim -5.7 \pm 0.4$ GPa) measured at room temperature on an alumina scale grown at 1100 °C on a bare MCrAlY corresponded to the calculated thermal stresses; this means that the level of oxide growth stress, at the oxidation temperature, is likely to be lower than the flow stress of alumina at this temperature. It is thought therefore that plastic deformation inside the scale could occur during cooling, at intermediate temperatures, as a result of thermal stresses. According to Castaing *et al.* [13] the flow stress associated with prismatic slip varies from about 500 MPa to 1 GPa when the temperature varies between 1200 and 900 °C. Another possible cause for the generation of dislocations inside the alumina layer

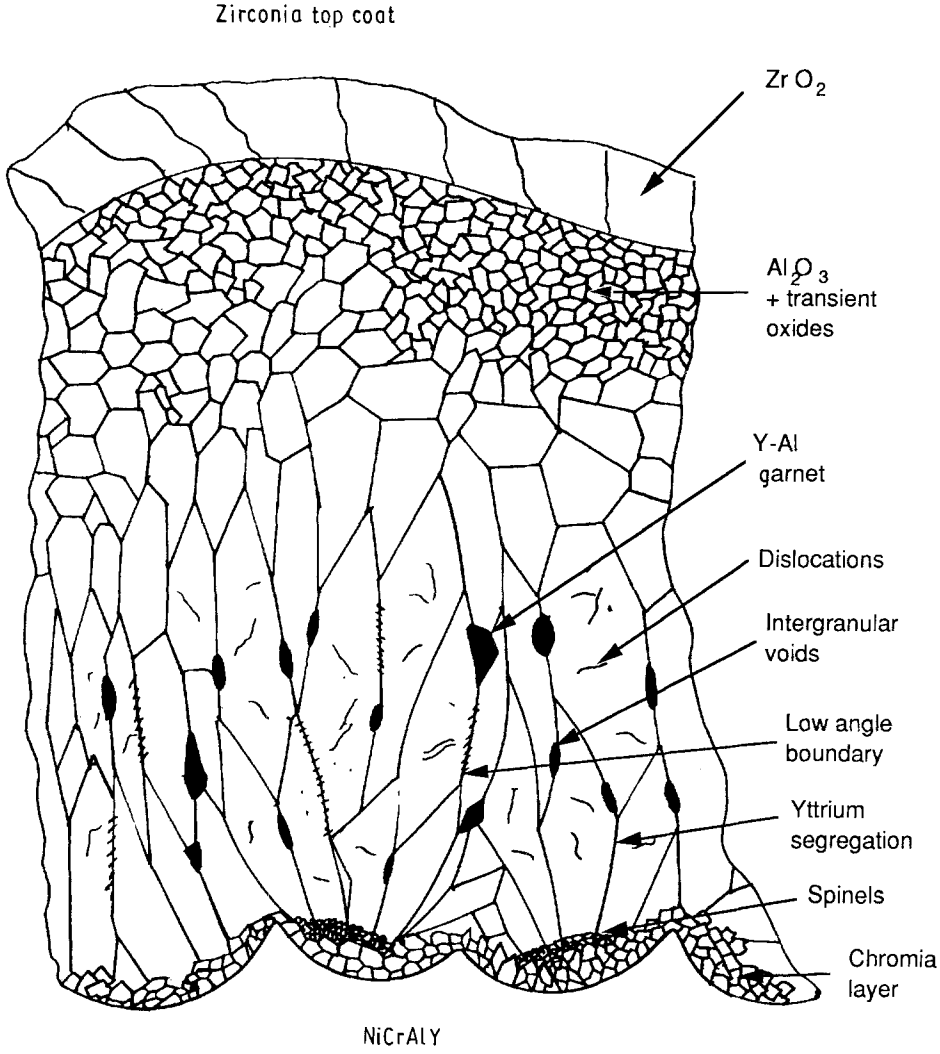

Figure 10 Schematic representation of the microstructural features present in the oxide scale grown during 100 h at 1200 °C at the ZrO_2–NiCrAlY interface.

could be a stress relaxation phenomenon occurring during sample thinning the sample.

5. Conclusion

The microstructure of oxide scales grown at 1100 and 1200 °C at the NiCrAlY–zirconia interface of thermal barrier coatings has been studied by classical and analytical transmission electron microscopy, on transverse cross-sections as well as by high-resolution SIMS. The oxide grain morphology, comparable to that of alumina scales grown on bare MCrAlY at 1100 °C, is typical of oxide growth at the metal–oxide interface, suggesting that the scale mainly forms by oxygen grain-boundary diffusion. Segregation of yttrium at oxide grain boundaries has been observed, leading us to think that yttrium segregation has enhanced oxygen diffusion. Significant amounts of zirconium inside the alumina grains have also been observed, sustaining the hypothesis that the oxide scale has also partially grown by reduction of the zirconia top-coat. The large quantities of defects observed in the alumina scale formed at 1200 °C prove that at high temperatures, a significant plasticity of yttrium, zirconium and chromium-doped alumina can be obtained.

Acknowledgements

The authors gratefully acknowledge the help of F. Hillion for experimental SIMS analysis and J. L. Pouchou for EDS spectra interpretation.

References

1. R. A. MILLER, J. L. SMIALEK and R. G. GARLICK, in "Advances in Ceramics", Vol. 3, edited by A. H. Heuer and L. W. Hoobs (American Ceramic Society, Colombus, Ohio, 1981) pp. 241–251.
2. S. STECURA, NASA Technical Memorandum 86905 (1985).
3. J.-M. VEYS, A. RIVIÈRE and R. MÉVREL, in Proceedings of First Plasma-Technik Symposium, Lucerne, 1988, Vol. 2, edited by H. Eschnauer, pp. 115–124.
4. P. CHOQUET and R. MÉVREL, *Mater. Sci. Engng* **A120/A121** (1989) 153.
5. C. DIOT, P. CHOQUET and R. MÉVREL, in Proceedings of International Conference on Residual Stresses, Nancy, France, November 1989, Vol. 2, Elsevier, pp. 273–278.
6. T. E. RAMANARAYANAN, M. RAGHAVAN and R. PETKOVIC-LUTON, *J. Electrochem. Soc.* **131** (1984) 923.
7. D. S. SHUR, PhD Thesis, Case Western Reserve University, USA (1984).
8. G. TRÉMOUILLE, J-L. DEREP and R. PORTIER, in Proceedings of 11th International Thermal Spraying Conference, Montreal, Canada, September 1986, pp. 445–454.
9. W. E. KING, N. L. PETERSON, and J. F. REDDY, in

Proceedings of International Congress on Metallic Corrosion, Toronto, Canada, June 1984, pp. 4–28.
10. L. LELAIT, S. ALPÉRINE, C. DIOT and R. MÉVREL, *Mater. Sci. Engng* **A120/A121** (1989) 475.
11. G. SLODZIAN, B. DAIGNE, F. GIRARD and F. BOUST, in Proceedings of 6th International Conference on Secondary Ion Mass Spectrometry, Versailles, France, September 1987, edited by A. Benninghoven *et al.* (Wiley), pp. 189–192.
12. P. CHOQUET, Thèse d'état, Orsay, France (1988).
13. P. CASTAING, J. CADOZ and S. H. KIRBY, *J. Phys.* **42** (1981) 3–6.

Received 14 November 1990
and accepted 10 April 1991